

Experimental Real-Time Phase Synchronization of a Paced Chaotic Plasma Discharge

Catalin M. Ticos, Epaminondas Rosa, Jr., William B. Pardo, Jonathan A. Walkenstein, and Marco Monti

Nonlinear Dynamics Laboratory, Department of Physics, University of Miami, Coral Gables, Florida 33146

(Received 10 April 2000)

Experimental phase synchronization of chaos in a plasma discharge is studied using a phase variable lift technique (i.e., phase points separated by 2π are not considered as the same). Real-time observation of synchronized and unsynchronized states is made possible through a real-time sampling procedure. Parameter space regions of synchronization and unsynchronization are identified, and a set of equations is suggested to model the real plasma circuit.

PACS numbers: 05.45.Xt, 52.35.Ra

Given a chaotic oscillator for which an angle coordinate can be suitably introduced as a state space variable, it is often the case that the phase of this oscillator synchronizes with the phase of an external periodic perturbation, or pacer [1]. That is, the phase difference between the chaotic oscillator and the pacer remains bounded by some appropriate constant fraction of 2π for *all time*, depending on the values of the amplitude and frequency of the pacer [2]. In this phase synchronized state, the oscillator remains chaotic, but its phase is in step with that of the pacing signal.

Phase synchronization is an important feature associated with chaos in a number of situations including communication using the natural symbolic dynamics of chaos [3], lasers [4], paddlefish electrosensitive cells [5], cardiac muscle pacing [6], coupled chaotic neurons [7], and plasmas [8]. In particular, plasma light intensity oscillations, often called striations, have been observed since the early days of plasma discharges. More recently, the chaotic nature of these oscillations (period doubling route to chaos and current bifurcation, for example) has been studied both experimentally and numerically [9]. Much effort has been devoted to the control of the chaotic behavior of gas discharges, either by varying different parameters such as the voltage, load resistance, and pressure, or by driving the plasma with periodic external sources [10].

In this Letter we present experimental results of real-time phase synchronization of chaos. To the best of our knowledge, this is the first real time demonstration of phase synchronization of a chaotic plasma discharge tube subject to the action of a periodic wave generator. Under certain conditions, the motion of the chaotic attractor constructed from current intensity measurements is such that the trajectory of the system continually circulates around one of the Cartesian axes. In this case, an angle coordinate can be introduced as a state space variable and regarded as the oscillator phase. The power spectrum of the signal is broad with a peak clearly indicating the existence of a dominant frequency [8]. Paced with a sinusoidal voltage with amplitude 0.4 V (small compared to the 850 V applied across the tube) and frequency close to the dominant frequency of the plasma, the phase of the system locks

up for long time intervals with the phase of the sinusoidal signal. Our study uses a “lift” of the oscillator phase variable where points separated by 2π are not considered as the same. For example, the xy projection of the attractor of the Rössler system $\dot{x} = -(y + z)$, $\dot{y} = x + 0.25y$, $\dot{z} = 0.90 + z(x - 6.0)$ resembles a smeared circle with the orbit continually circulating around the z axis. Trajectory stroboscopic surfaces of section taken at the dominant frequency of the oscillator are depicted in Fig. 1(a) as dots scattered all over the attractor due to phase diffusion [2]. However, if we add the term $A \sin 2\pi t/T$ to the right-hand side of the second Rössler equation, with appropriate values for the amplitude A and frequency $f = 1/T$,

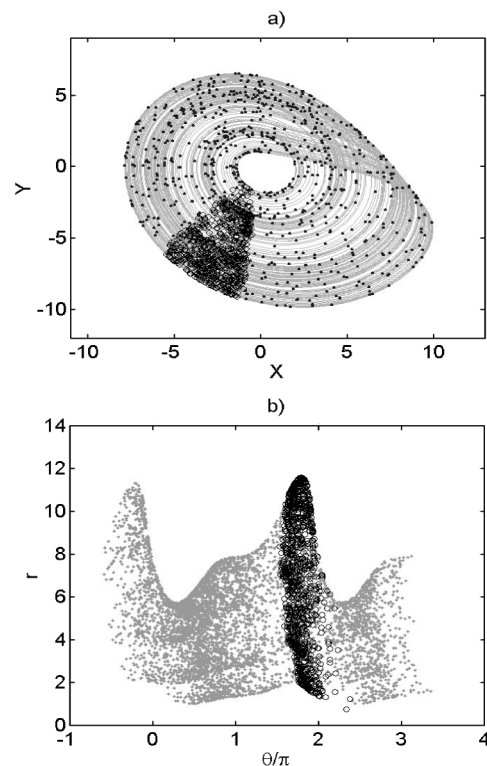


FIG. 1. (a) Projection of the Rössler attractor in Cartesian coordinates, and (b) cylindrical coordinates. In both cases, dots correspond to phase unsynchronization and empty circles correspond to phase synchronization.

the phase of the oscillator synchronizes with the phase of the pacer. Stroboscopic sampling in this regime is shown in Fig. 1(a) as open circles, confined into a small region of the attractor due to phase synchronization. A different view of this phenomenon can be obtained using cylindrical coordinates with the transformation $(x, y, z) \rightarrow (r, \phi, z)$, where $r = \sqrt{x^2 + y^2}$ and $\phi = \arcsin(y/r)$. By regarding ϕ as continuous in time, points separated by 2π are shown 2π apart along the angle coordinate real line. The phase difference between the oscillator and the pacer, $\theta = \phi - 2\pi t/T$, also continuous in time, is defined on the real line $-\infty < \theta < +\infty$ (rather than on the circle $0 \leq \theta \leq 2\pi$). This phase lift allows us to see phase synchronization as a chaotic attractor with extension in θ less than 2π . Stroboscopic sampling of the *unpaced* system generates points lying on a branched manifold that spreads along the θ real line, shown as gray dots in Fig. 1(b). Stroboscopic sampling of the *paced* system also generates points lying on a branched manifold, but these points do not fill the entire manifold. In the synchronized state, the strobed attractor is localized within a small interval in θ as indicated by the open circles in Fig. 1(b).

The phase lift technique briefly described above is now applied to our experimental realization depicted in Fig. 2. It includes an unmagnetized plasma produced in a sealed glass cylindrical envelope with a central capillary region and a wider diameter at the ends where the electrodes are located (Geissler tube). The tube is filled with spectroscopically pure helium gas [11]. The anode and the cathode of the tube are connected to a high dc voltage (850 V) through a current limiting resistor $R = 30 \text{ k}\Omega$. In parallel with the resistor, a capacitor $C = 3.5 \text{ pF}$ cuts out the high voltage and a transformer picks up a low amplitude (0.4 V) pacing sine wave from a function generator. The signal output is provided by a current probe. After amplification, the current is passed in parallel to an analog derivative circuit, a PC based GPIB controller CAMAC crate, and an oscilloscope. For the data acquisition, we use a LeCroy 6810 Wave Form Recorder. The attractor can be viewed real time on the oscilloscope by plotting the raw signal output versus its analog derivative. The Lyapunov spectrum

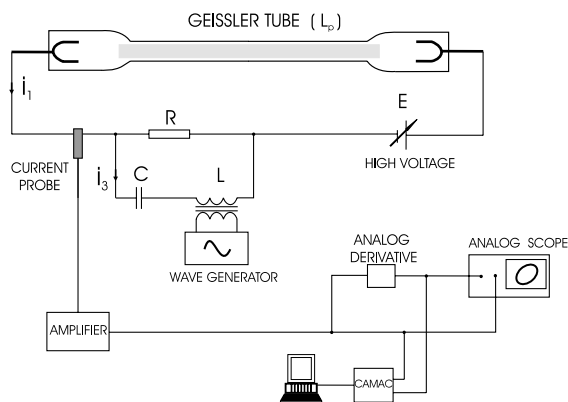


FIG. 2. Schematic representation of our experimental setup.

of the acquired signal provides a quantitative measure of the system sensitivity to small perturbations. For the experimental setup as above, with a voltage across the tube of 850 V and no pacing, we obtain $\lambda_1 \approx 0.36$, $\lambda_2 \approx 0.00$, and $\lambda_3 \approx -0.74$, for a sampling interval of $5 \mu\text{s}$ [12]. The corresponding Lyapunov dimension [13] is $d_L \approx 2.49$.

One way of verifying phase synchronization is by acquiring a long signal with the wave generator off, reconstructing the attractor, and treating the time series data in the same manner as done above for the Rössler system. The power spectrum of the signal is wide with a dominant frequency of 6960 Hz. We use this frequency to take stroboscopic surfaces of a section of the (unpaced) signal and plot the result in Fig. 3(a) as dots on top of the attractor (gray continuous line). Notice the spread of points all over the attractor, a consequence of the phase unsynchronized state of the system. However, an entirely different result is obtained when the plasma is paced with a sine wave with frequency of 6960 Hz and amplitude of 0.4 V. The same stroboscopic procedure described above produces points restricted within a small region of the attractor as denoted by the open circles in Fig. 3(a), indicating phase synchronization. Following exactly the same steps as above for the Rössler numerical example, we move from Cartesian coordinates in Fig. 3(a) to cylindrical coordinates in Fig. 3(b) by applying the transformation $(x, y, z) \rightarrow (r, \phi, z)$, etc. The *unpaced* plasma attractor along the θ real line is

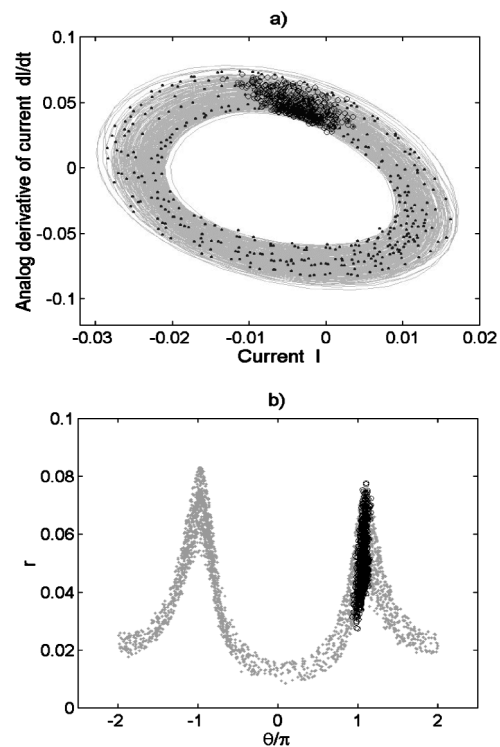


FIG. 3. (a) Projection of the plasma attractor in Cartesian coordinates, and (b) cylindrical coordinates. In both cases, dots correspond to phase unsynchronization and empty circles correspond to phase synchronization.

represented by the gray dots in Fig. 3(b) [14]. This corresponds to a phase unsynchronized state of the plasma depicted by the spread of points along the θ line. An identical procedure applied to the *paced* plasma generates the points plotted as open circles, in this case concentrated within a small region around $\theta = \pi$. This localized strobed attractor is a representation of the synchronized state of the paced plasma.

Another way of verifying phase synchronization, in this case real time, is by sampling the measured signal of the paced plasma with a sampling rate equal to the dominant frequency of the signal (same as the pacer frequency). This is achieved by using a PCI-MIO 16E4 National Instruments board connected to a computer, with two programs running simultaneously: one shows the power spectrum of the signal and the other shows the attractor. We tune the wave generator to the frequency given by the peak in the power spectrum (6960 Hz in this case) after which we sample the attractor at the same frequency. The image displays dots concentrated within a small region shown in Fig. 4(a) for the phase synchronized regime (amplitude $A = 0.4$ V), as opposed to dots spread over a larger region shown in Fig. 4(b) for phase unsynchronization (amplitude $A = 0.1$ V).

This diagnostics for verifying phase synchronization provides us with a useful tool for checking, in real time, the regime corresponding to different values of pacer amplitude A and pacer frequency f . Figure 5 shows parameter space (A, f) regions of phase synchronization (open circles) and phase unsynchronization (filled circles) that were determined using this technique. The synchronized states within the tongue are very stable for long periods of time. Notice that the study of Ref. [2] names unsynchronization the states where the system sustains epochs, possibly long, of synchronized state interrupted by short intervals where the phase of the pacer undergoes a 2π slip behind (or ahead of) the oscillator [15]. This is not the case in our experimental system, except for a few points in the neighborhood of the boundary between synchronized and unsynchronized states of Fig. 5. The phase unsynchronization region represented in Fig. 5 (filled circles) corresponds to states of the system where

our measurements do not detect epochs of synchronization separated by short intervals of 2π phase slip. These are states where the plasma frequency seems to be not correlated with the periodic pacing wave and the sampled points spread all over the attractor [dots of Fig. 3(a)]. However, a behavior somewhat similar to the numerical results of Ref. [2] is observed at the boundary between synchronization and unsynchronization regions. We noticed a few cases in which the system stays synchronized for a while, becomes unsynchronized, and goes back to synchronization again [16].

A precise mathematical model for our plasma system requires a detailed and comprehensive study of the complicated discharge kinetics. Still, we can treat the plasma dynamically as a nonlinear circuit element, and produce a set of three differential equations with two currents and one voltage as variables. This is consistent with present and previous observations showing low dimensionality in plasmas [9–11], indicating that the system should be described by a set of autonomous differential equations with at least three independent variables. The circuit depicted in Fig. 2 behaves as an electrical relaxation oscillator due to the presence of the capacitor C , and of the Geissler discharge tube with a nonlinear characteristic $V(I)$. We model this nonlinear element as an idealized voltage-current characteristic that consists of a broken line with two negative slopes. In our idealized element, we consider only the region of luminous discharge, starting at small currents (microamps which we approximate as zero). After ignition, the concentration of free charge carriers builds up leading to a current intensity increase a few orders of magnitude. The voltage necessary to sustain the discharge drops accordingly, and the running point of the system jumps to a higher current. Here the system evolves on the second region of the characteristics with a less steep negative slope. The inductance L supplies more feedback into the circuit [17], and the inductance L_P accounts for both the parasitic inductance and inertial effects within the tube. We apply Kirchoff's law on two loops of the circuit shown in Fig. 2: the plasma-resistor-source loop and the resistor-capacitor-inductor loop. The resulting

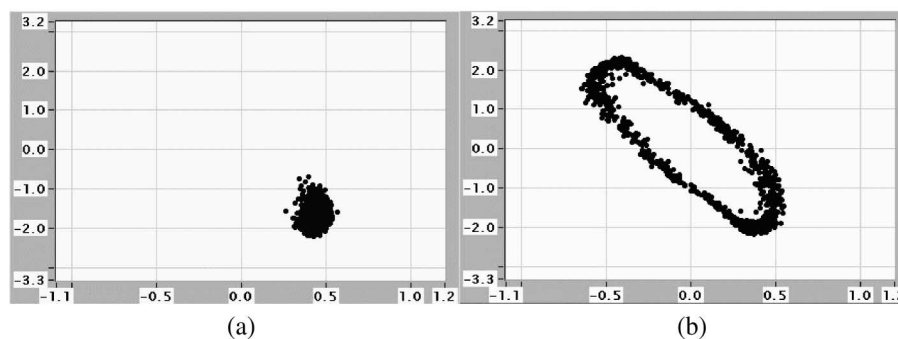


FIG. 4. Real time experimental observation of (a) phase synchronization with pacer amplitude $A = 0.40$ V, and (b) phase unsynchronization with pacer amplitude $A = 0.10$ V.

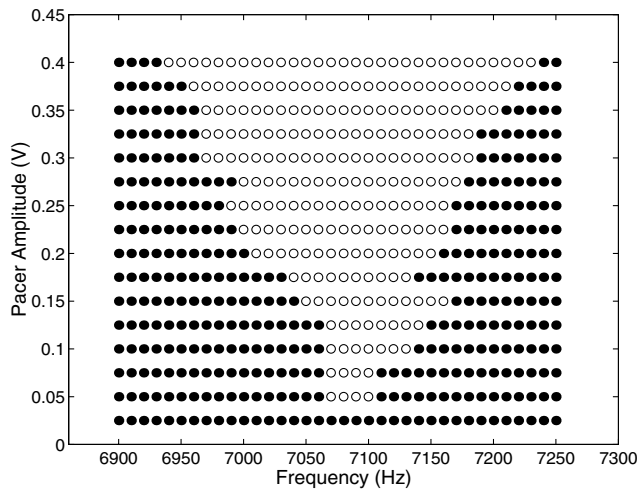


FIG. 5. Amplitude A and frequency f values for phase synchronized plasma (open circles) and phase unsynchronized plasma (filled circles).

equations are $L_P \frac{dI_1}{dt} = E - RI_2 - V_P(I_1)$ and $L \frac{dI_3}{dt} = RI_2 - \int \frac{I_3}{C} dt$, where the integral term is identified with the voltage across the capacitor. We write $v = -\int \frac{I_3}{C} dt$, and the time derivative of v provides us with a third equation $\frac{dv}{dt} = -\frac{I_3}{C}$. Straightforward algebra yields $\dot{x} = \alpha \frac{E}{R} - \alpha(x - y) - \frac{\alpha}{R} V_P(x)$, $\dot{y} = x - y + z$, and $\dot{z} = -\beta y$, where $x = I_1$, $y = I_3$, $z = \frac{v}{R}$, $\alpha = \frac{L}{L_P}$, $\beta = \frac{L}{R^2 C}$, and $V_P(x) = 0$ for $x < 0$

$$= 1000 + m_1 x \quad \text{for } 0 \leq x < 2.6 \text{ mA}$$

$$= 1000 + m_0 x + 2.6(m_1 - m_0) \quad \text{for } x \geq 2.6 \text{ mA}.$$

The numerical values corresponding to our experiment are $L = 32$ mH, $L_P = 4$ mH, $C = 3.5$ pF, $E = 850$ V, and $R = 30$ k Ω . The slopes are $m_1 = -7.46$ V/mA, and $m_0 = -136.53$ V/mA. These equations, as presented, are similar to the equations of the Chua circuit [18], and produce a single spiral Rössler-like attractor. In a future publication [16], we provide a more detailed analysis of the model and its connection with the real experimental setup. This idealized model, for example, does not take into account the hysteretic behavior of the current I -voltage V_P characteristic. It is well known that dc glow discharges produced in gases at low pressure, or thermoionic discharges, show an oscillatory behavior when their running point is on the negative slope of the voltage-current characteristic [19].

[1] A. S. Pikovsky, Sov. J. Commun. Technol. Electron. **30**, 85 (1985); E. F. Stone, Phys. Lett. A **163**, 367 (1992); A. S. Pikovsky, M. G. Rosenblum, G. V. Osipov, and J. Kurths, Physica (Amsterdam) **104D**, 219 (1997); T. Yalçinkaya and Y.-C. Lai, Phys. Rev. Lett. **79**, 3885 (1997).

[2] E. Rosa, Jr., E. Ott, and M. H. Hess, Phys. Rev. Lett. **80**, 1642 (1998).

[3] E. Rosa, Jr., S. Hayes, and C. Grebogi, Phys. Rev. Lett. **78**, 1247 (1997); L. M. Pecora, T. L. Carroll, G. Johnson, and D. Mar, Phys. Rev. E **56**, 5090 (1997).

[4] P. M. Varangis, A. Gavrielides, T. Erneux, V. Kovanis, and L. F. Lester, Phys. Rev. Lett. **78**, 2353 (1997); J. R. Terry, K. S. Thornburg, Jr., D. J. DeShazer, G. D. Vanwiggeren, S. Zhu, P. Ashwin, and R. Roy, Phys. Rev. E **59**, 4036 (1999).

[5] A. Neiman, X. Pei, D. Russel, W. Wojtenek, L. Wilkens, F. Moss, H. A. Braun, M. T. Huber, and K. Voigt, Phys. Rev. Lett. **82**, 660 (1999).

[6] G. M. Hall, S. Bahar, and D. J. Gauthier, Phys. Rev. Lett. **82**, 2995 (1999); A. R. Yehia, D. Jeandupeux, F. Alonso, and M. R. Guevara, Chaos **9**, 916 (1999).

[7] J.-W. Shuai and D. M. Durand, Phys. Lett. A **264**, 289 (1999).

[8] E. Rosa, Jr., W. B. Pardo, C. M. Ticos, J. A. Walkenstein, and M. Monti, Int. J. Bifurcation Chaos Appl. Sci. Eng. (to be published).

[9] C. Wilke, R. W. Leven, and H. Deutsch, Phys. Lett. A **136**, 114 (1989); T. Braun, J. A. Lisboa, and J. A. C. Gallas, Phys. Rev. Lett. **68**, 2770 (1992); D. Weixing, H. Wei, W. Xiaodong, and C. X. Yu, Phys. Rev. Lett. **70**, 170 (1993); M. Sanduloviciu, V. Melnig, and C. Borcia, Phys. Lett. A **229**, 354 (1997); T. Kajiwara and M. Sano, Jpn. J. Appl. Phys. **38**, 918 (1999).

[10] P. Y. Cheung, S. Donovan, and A. Y. Wong, Phys. Rev. Lett. **61**, 1360 (1988); T. Klinger, F. Greiner, A. Rhode, and A. Piel, Phys. Plasmas **2**, 1822 (1995); T. Mausbach, T. Klinger, and A. Piel, Phys. Plasmas **6**, 3817 (1999).

[11] J. A. Walkenstein, W. B. Pardo, M. Monti, R. E. O'Meara, T. N. Buch, and E. Rosa, Jr., Phys. Lett. A **261**, 183 (1999). This reference presents a detailed study of plasma spatiotemporal behavior due to the geometry of the tube and finite length of the discharge, as opposed to the present Letter which displays results of temporal chaos in a commercial Geissler tube.

[12] H. D. I. Abarbanel, *Analysis of Observed Chaotic Data* (Springer-Verlag, New York, 1996); R. Hegger and H. Kantz, Chaos **9**, 413 (1999); <http://www.physics.gatech.edu/chaos>.

[13] P. Frederickson, J. L. Kaplan, E. D. Yorke, and J. A. Yorke, J. Differ. Equ. **49**, 185 (1985).

[14] Figure 3(b) is obtained from Fig. 3(a) in exactly the same way as Fig. 1(b) is obtained from Fig. 1(a). Figures 3(a) and 3(b) are the experimental equivalent of the numerical results shown in Figs. 1(a) and 1(b), respectively.

[15] K. J. Lee, Y. Kwak, and T. K. Lim, Phys. Rev. Lett. **81**, 321 (1998); M. A. Zaks, E.-H. Park, M. G. Rosenblum, and J. Kurths, Phys. Rev. Lett. **82**, 4228 (1999).

[16] W. B. Pardo, E. Rosa, Jr., C. M. Ticos, J. A. Walkenstein, and M. Monti (to be published).

[17] E. A. Jackson, *Perspectives of Nonlinear Dynamics* (Cambridge University Press, New York, 1991), Vol. 1.

[18] T. Matsumoto, L. O. Chua, and M. Komuro, IEEE Trans. Circuits Syst. **32**, 798 (1985).

[19] M. P. Kennedy and L. O. Chua, IEEE Trans. Circuits Syst. **33**, 947 (1986); J. Qin, L. Wang, D. P. Yuan, P. Gao, and B. Z. Zhang, Phys. Rev. Lett. **63**, 163 (1989); T. Hayashi, Phys. Rev. Lett. **84**, 3334 (2000).